Research Article | Vol. 12, No. 11 / 1 Nov 2021 / Biomedical Optics Express 7122
Biomedical Optics EXPRESS

Effects of high intensity non-ionizing terahertz radiation on human skin fibroblasts

DMITRY S. SITNIKOV,[1,*] INNA V. ILINA,[1] VERONIKA A. REVKOVA,[2] SERGEY A. RODIONOV,[3] SVETLANA A. GUROVA,[4] RIMMA O. SHATALOVA,[4] ALEXEY V. KOVALEV,[3] ANDREY V. OVCHINNIKOV,[1] OLEG V. CHEFONOV,[1] MIKHAIL A. KONOPLYANNIKOV,[2,5] VLADIMIR A. KALSIN,[2] AND VLADIMIR P. BAKLAUSHEV[2]

[1] *Joint Institute for High Temperatures of the Russian Academy of Sciences, Moscow, Russia*
[2] *Federal Research and Clinical Center of Specialized Medical Care and Medical Technologies FMBA of Russia, Moscow, Russia*
[3] *N. N. Priorov National Medical Research Center of Traumatology and Orthopedics, Moscow, Russia*
[4] *National Research nuclear University MEPhI Obninsk Institute for Nuclear Power Engineering, Obninsk, Russia*
[5] *Institute for Regenerative Medicine, Sechenov First Moscow State Medical University, Moscow, Russia*
[*] *Sitnik.ds@gmail.com*

Abstract: For the first time, the data have been obtained on the effects of high-intensity terahertz (THz) radiation (with the intensity of 30 GW/cm^2, electric field strength of 3.5 MV/cm) on human skin fibroblasts. A quantitative estimation of the number of histone H2AX foci of phosphorylation was performed. The number of foci per cell was studied depending on the irradiation time, as well as on the THz pulse energy. The performed studies have shown that the appearance of the foci is not related to either the oxidative stress (the cells preserve their morphology, cytoskeleton structure, and the reactive oxygen species content does not exceed the control values), or the thermal effect of THz radiation. The prolonged irradiation of fibroblasts also did not result in a decrease of their proliferative index.

1. Introduction

Terahertz (THz) radiation belongs to the non-ionizing radiation (NIR) type and is ranged from 0.3 to 10 THz, in between the microwave and infrared regions. With the development of new techniques for the generation and detection of THz radiation, the spectrum of its applications in spectroscopy and microscopy modalities has expanded, covering characterization of antibacterial surfaces [1], label-free diagnosis of malignant and benign neoplasms [2–4] and cell identification [5,6]. However, in spite of the tremendous interest, which has arisen in the scientific community, the issue of the radiation safety is still discussed, especially when speaking about high-intensity sources. In her recent review [7], M. Havas casts some doubt on the widely spread statement that "since NIR does not have enough energy to dislodge electrons, it is unable to cause cancer" and brings arguments against it. It is stated that (1) mechanisms of biological interactions are different for ionizing radiation (IR) and NIR; (2) there is sufficient evidence of cell damage caused by NIR at levels well below thermal guidelines; (3) various mechanisms that involve oxidative stress and can account for the increase in tumors under exposure to low frequency or radio frequency electromagnetic radiation have been reported. Unfortunately, many countries set standards based on the false assumption that there are no adverse health effects of radio frequency (RF) radiation other than those that are caused by tissue heating [8]. By now, the effect of RF radiation including phone-frequencies on biological objects has been fairly well studied. It has been shown [8]

#440460 https://doi.org/10.1364/BOE.440460
Journal © 2021 Received 13 Aug 2021; revised 6 Oct 2021; accepted 19 Oct 2021; published 26 Oct 2021

Biomedical Optics EXPRESS

that the mechanism(s) of interaction include induction of reactive oxygen species (ROS), gene expression alteration and DNA damage through both epigenetic and genetic processes.

As for NIR of the THz spectrum, the subject of this study, a large volume of experimental results has been collected, some of them demonstrating the absence of cell changes caused by non-ionizing THz radiation and some demonstrating the presence of such changes (in particular, changes in gene expression, permeability of membranes or the number of micronuclei in cells, as well as DNA damage or demethylation, see the studies and reviews [9–17] for details). However, the essential differences in the experimental parameters, including the duration of exposure, power and frequency of THz radiation, hinder the systematization of the results and their theoretical justification.

According to prediction [18] that either linear or non-linear resonant interaction between DNA and intense THz radiation may cause local rupture of hydrogen bonds in double-stranded DNA chains, the issue of genotoxicity has become of a primary significance with the appearance of high-intensity sources of pulsed THz radiation. Recently, histone H2AX phosphorylation has become one of the most sensitive biomarkers to evaluate genotoxicity [19]. Histone proteins participate in the DNA packing and arrangement in chromatin in eukaryotes. Epigenetic alterations in histones (acetylation, methylation, phosphorylation etc.) change the DNA accessibility for transcription and may play a key role in the malignant transformation of cells, as well as in the resistance of tumors to drugs [20]. Such alterations have a reversible character and may be caused both by individual genes' mutations and by the environmental effects.

The histone H2AX phosphorylation on serine 139 was discovered in cells exposed to ionizing radiation [21]. Later, a series of studies had shown that the number of γH2AX foci was associated with DNA double-strand breaks (DSB) and depended on the dose of ionizing radiation [22–25]. In the case of non-ionizing radiation, for example, of the ultraviolet or microwave spectral range, the formation of γH2AX foci is frequently related not to double-strand DNA breaks, but to other causes [26–29]. The observed increase of γH2AX foci is caused by the altered chromatin structure associated with the thermal effect, among other factors. Not only the chromatin structure alteration [30], but also a number of other endogenous processes may result in the formation of γH2AX foci, in particular: cell ageing [31], oxidative stress [32], and also processes associated with the cell cycle.

To date, rather contradictory data have been collected on the influence of THz NIR on the formation of histone H2AX phosphorylation foci. While a qualitative analysis [33] showed the induction of H2AX phosphorylation after exposure to intense THz pulses for 10 minutes, a quantitative analysis performed in [28,34,35] did not reveal such changes.

This study is dedicated to the molecular-cellular mechanisms of the human skin fibroblasts' reaction to high-intensity pulsed THz radiation. For the first time, dependence of the number of γH2AX foci on exposure duration has been obtained. Post-irradiation kinetics of γH2AX foci numbers has also been studied. We have analyzed a number of factors capable of initiating the formation of histone H2AX phosphorylation foci in human skin fibroblasts exposed to high-intensity non-ionizing pulsed radiation of the THz range.

2. Materials and methods

2.1. THz exposure set-up

Optical rectification of laser pulses is an efficient technique for generating THz radiation. A series of organic crystals such as DAST [4-N-methylstilbazolium tosylate], DSTMS [4-N,N-dimethylamino-4′-N′-methyl-stilba- zolium 2,4,6-trimethylbenzenesulfonate], and OH1 [(2-(3-(4-hydroxystyryl)-5,5-dimethylcyclo- hex-2-enylidene) malononitrile] demonstrate a high conversion efficiency (up to 3%) through pumping with near-infrared femtosecond laser pulses [36]. A nonlinear OH1 organic crystal with a diameter of 6 mm and a thickness of 420 ± 10 μm (Rainbow Photonics, Switzerland) was used in the experimental setup (Fig. 1(a)) to generate THz

Biomedical Optics EXPRESS

pulses. It was pumped by pulses from a Cr:forsterite laser system supplied with a multipass amplifier operating at 100 Hz (Avesta Project LLC, Russia) [37] and emitting 100 fs pulses at a wavelength of 1024 nm with the energy of 1.1 ± 0.05 mJ. The laser pump radiation was cut off by a LPF8.8-47 THz filter (Tydex LLC, Russia) with 70% transmission in the THz spectral range, placed behind the crystal. The energy of THz pulses after the filter, $E_{\mathrm{THz}} = 18 \pm 0.5$ μJ was measured by a calibrated Golay cell (a GC-1D optoacoustic detector, Tydex LLC, Russia). To expand the THz beam, a telescope consisting of two off-axis parabolic mirrors (with the reflected focal lengths of 15 mm and 152.4 mm) was assembled after the OH1 crystal. The THz radiation was focused to a spot with diameter of 480 μm at $1/e$ level by an off-axis parabolic mirror (MPD229H-M01, Thorlabs, USA) with a reflected focal length and a diameter of 50.8 mm. The pulse duration was measured using a well-known electro-optic sampling technique. A waveform and a spectrum (obtained by calculating the Fourier transform of the waveform) of a THz pulse are presented in Figs. 1(b) and 1(c). The Gaussian envelope approximation of the registered electric field waveform is generally used to determine the duration, which equals $\tau_{\mathrm{THz.E}} = 685$ fs as a full width at half maximum (FWHM). Generally, the pulse duration implies the value of the intensity profile (not the field one), thus, the presented Gaussian function should be squared. The duration of a THz pulse is then equals $\tau_{\mathrm{THz.I}} = \tau_{\mathrm{THz.E}}/\sqrt{2} = 484$ fs.

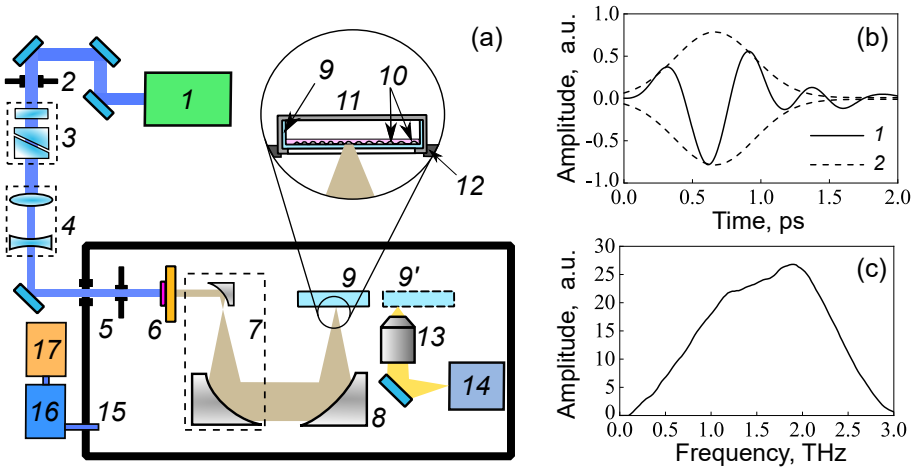

Fig. 1. (a) Experimental setup for cell irradiation: *1* – femtosecond laser system, *2*, *5* – iris diaphragms, *3* – attenuation unit, *4* – lens telescope, *6* – OH1 crystal with THz filter, *7* – mirror telescope (1:10), *8* – focusing parabolic mirror, *9* and *9'*– Petri dish in "THz" or "video" channels, *10* – cells, *11* – heating plate with a lid, *12* – 3D motorized translation stage, *13* – microobjective, *14* – CCD-camera, *15* – dried box, *16* – adsorption dryer, *17* – air compressor; (b) Waveform of the THz pulse: *1* – electric field waveform, *2* – Gaussian envelope; (c) Spectrum of the THz pulse. The peak intensity and electric field strength of THz pulses were estimated to be 32 GW/cm^2 and 3.5 MV/cm, correspondingly. The spectral bandwidth of up to 3 THz with central frequency close to 1.5 THz was measured.

The cell exposure was performed by focusing the THz radiation through the bottom of a plastic dish with a cell monolayer attached and filled with culture medium. A standard 35-mm Petri dish was placed in an incubating plate with a lid (heating system, Ibidi) for long-term cell irradiation mounted on a 3-dimentional motorized linear stage (8MT167-100 along X and Y axes, 8MT173-20 along Z axis, Standa). A video-channel consisting of a 20× microobjective with a numerical aperture NA=0.4 and a CCD-camera was assembled to control the position of the dish with respect to the focal plane of the focusing parabolic mirror. The Petri dish could be

Biomedical Optics EXPRESS

moved along X axis to either "THz" or "video" channels. Cells clearly visible by camera were considered to be in the THz beam waist plane.

To minimize the absorption of THz radiation by water vapour, the entire experimental setup (see [38] for details) was assembled in a sealed box purged with dry air. Five minutes were typically required for an air compressor (SB4-100.OLD15 T, Remeza) and an adsorption dryer (ADS3, Ceccato) to reduce locally the relative humidity of the air to 2-3%.

Taking into account the transmission values T_a of the air along the pathway and T_d of the plastic dish, the peak intensity of the THz pulse entering the culture medium can be estimated as (henceforth * denotes a parameter of the pulse entering the culture medium):

$$I^*_{THz}=\frac{4}{\pi}\frac{T_a \cdot T_d \cdot E_{THz} \cdot k}{d^2_{1/e} \cdot \tau_{THz.I}} \tag{1}$$

where T_a is taken equal to 0.95 for the 2% relative humidity maintained in the box during cell irradiation experiments, $T_d = 0.89$ [38] for the dish (#80466, ibidi) with a 180 μm thick polymer bottom, $d_{1/e} = 480$ μm is the diameter of the focused THz beam at the $1/e$ level, $\tau_{THz.I}$ is the duration (FWHM) of a THz pulse, $k = 1.86$ is the correction coefficient calculated as a ratio of the area under the Gaussian curve in Fig. 1(b) to the area under the THz waveform profile (see [39] for details). For optical pulses with the carrier frequency of 10^{14} Hz the fill factor of the Gaussian envelop is close to unity ($k \approx 1$) and no correction is required.

The THz electric field strength is given by

$$W^*_{THz}=\sqrt{\frac{I^*_{THz}}{\varepsilon_0 c}}, \tag{2}$$

where I^*_{THz} is the peak intensity of the THz pulse entering the culture medium, ε_0 is the dielectric permittivity, and c is the speed of light. The peak intensity and electric field strength of THz pulses were estimated to be I^*_{THz}=32 GW/cm^2 and $W^*_{THz} = 3.5$ MV/cm, correspondingly.

A distinguishing feature of the experimental setup is the combination of a high peak power of the THz source with a low average power. The former enables us to overcome the strong absorption of THz radiation by water, penetrate the culture medium (needed for the cell maintenance and viability) and reach the cells. The low average power is required to minimize the thermal effects induced in cells.

2.2. Cell exposure to THz radiation

This study was conducted in accordance with the Declaration of Helsinki and GCP guidelines and was approved by the local Ethical Committee of the Federal Research and Clinical Center of Specialized Medical Care and Medical Technologies (protocol No. 4/5 from December 2, 2019). The patient signed an informed consent before enrolling in this study.

The fibroblast primary cells culture was obtained by a biopsy of the behind-the-ear retroauricular skin regions as described previously [40,41]. The biopsy was performed from a healthy volunteer donor who signed the informed consent. To maximize the effect of THz radiation it was focused to a 480 μm-wide spot at the $1/e$ level. This means that the radiation intensity was the highest in the center of the beam and diminished along the radius to the level of $1/e$ from the maximum at the distance of 240 μm. Therefore, when evaluating the THz treatment effect, the analyzed field was limited by the 500 × 500 μm area. In order to simplify the identification of the area following the THz exposure, it was marked using laser engraving. The THz crystal and the THz filter were temporarily removed and an attenuated laser beam was focused on the bottom surface of the Petri dish. Laser marks of ~10 μm in the diameter were formed in the corners of a square (500 × 500 μm) to denote an area slightly wider than the size of the THz spot. Laser engraving was performed immediately before the experiment, after choosing the area with appropriate cell

Biomedical Optics EXPRESS

density to be exposed. The disadvantage of tight focusing of THz radiation is a small area of the irradiated surface and, correspondingly, a low number of treated cells. This circumstance restricts the choice of applied analytic techniques. In particular, such methods as flow cytometry demanding a high cell number ($\sim 10^6$) become unavailable, and the main technique used in this study was an immunocytochemical study.

The irradiation of cells was conducted in the close-to-natural conditions: the Petri dish was placed in a thermal chamber (heated plate and a lid) with a constant temperature of 37°C. The duration of the THz treatment varied in the experiment from 10 to 180 min. The cells in the adjacent well of the 4-well silicone insert in the ibidi dish were considered as a parallel control group.

2.3. Immunostaining for histone modifications and scoring of γH2AX foci

The cells were fixed 24 hours or immediately after the exposure in a Petri dish with a 4% paraformaldehyde solution containing 0.1% saponin in PBS (pH 7.4) for 20 min at room temperature, followed by two rinses in PBS and additional permeabilization with 0.5% Triton-X100 and 0.5% Tween 20 (in PBS, pH 7.4), supplemented with a 1% goat serum to block non-specific antibody binding. The fixed-permeabilized cells were then incubated for 1 h at 37°C with a primary rabbit polyclonal antibody against γH2AX (1 µg/ml, ab11174; abcam, USA). After three rinses with PBS, the cells were incubated for 1 h with secondary goat anti-rabbit IgG (H + L) antibodies (Alexa Fluor 488-conjugated, 5 µg/ml; Invitrogen, USA). Then, the Petri dishes were rinsed three times with DPBS. The cell nuclei were labeled with Hoechst 33342 stain (Thermo Fisher Scientific, USA). Immunofluorescence was analyzed using a Nikon A1 scanning laser confocal microscope (Nikon Co., Japan). The number of γH2AX foci was scored in all cell's nuclei in both the control and experimental groups.

2.4. ROS assay and f-actin visualization

To analyze reactive oxygen species (ROS) in cells exposed to THz radiation, a CM-H2DCFDA-based indicator was used (C6827, Thermo Fisher Scientific, USA). CM-H2DCFDA is a chloromethyl derivative of H2DCFDA, useful as an indicator for ROS in cells. CM-H2DCFDA passively diffuses into cells, where its acetate groups are cleaved by intracellular esterases and its thiol-reactive chloromethyl group reacts with intracellular glutathione and other thiols [42,43]. For a positive control, cells were incubated in a serum-free medium with added H_2O_2 for 30 min. Then the cells were rinsed twice with DPBS and incubated at 37°C in 5% CO_2 in the serum-free medium containing 20 µM CM-H2DCFDA for 1 h. After that the cells from the experimental group and the positive control cells were fixed with 4% paraformaldehyde in DPBS for 20 min at room temperature [44]. For F-actin visualization cells were rinsed twice in DPBS and permeabilized with 0.5% Triton-X100 and 0.5% Tween 20 (in PBS, pH 7.4), supplemented with Phalloidin–Tetramethylrhodamine B isothiocyanate (P1951, Sigma Aldrich, USA).

2.5. Heat shock proteins analysis

Cells exposed to THz radiation as well as cells from the positive control group (subjected to hyperthermia in a thermoshaker (at 42.5°C) for 1 hour) were fixed immediately with a 4% buffered paraformaldehyde solution as described above (section 2.3). The fixed-permeabilized cells were then incubated for 1 h at 37°C with a primary mouse monoclonal antibody against HSP70 (5 µg/ml, MS-482-B1, Thermo Fisher Scientific, USA) and stained with Alexa Fluor 488 secondary goat anti-mouse IgG (H + L) antibodies and Hoechst 33342 as described above (section 2.3). Immunofluorescence was analyzed using a Celena Digital imaging system (Logos biosystems, South Korea) and a Nikon A1 scanning laser confocal microscope (Nikon Co., Japan). Analysis area for the control group was chosen to be of the same cell density as in the THz treated area in the experimental dish.

Biomedical Optics EXPRESS

2.6. Proliferative index

Cells were fixed immediately after the exposure to THz radiation in a Petri dish with paraformaldehyde and stained with a primary rabbit polyclonal antibody against ki-67 (1 μg/ml, ab15580, Abcam, USA) and secondary Alexa Fluor 633 goat anti-rabbit IgG (H + L) antibodies as described above. Nuclear antigen ki-67 is expressed during various stages in the cell cycle and is widely used as cell proliferation marker in both research and cancer diagnostic settings [45,46]. The ki-67 proliferation index was calculated as a ratio of the ki67-positive cell number to the total number of Hoechst 33342-stained cells (percentage value). The immunofluorescence analysis was performed using a Nikon A1 scanning laser confocal microscope (Nikon Co., Japan).

2.7. Statistical analysis

To estimate the significance of the data, the experiment was repeated three times for each exposure time. There were usually 70-100 cells located in the irradiated area, so around 200-300 cells were analyzed for each time. The number of γH2AX foci per cell was counted as the total number of foci divided by the number of cells in the irradiated area. The statistical analysis of the histone H2AX phosphorylation foci formation was based on Fisher's one-way analysis of variance (ANOVA) with the probability of $p>0.05$**.** Fluorescence of stained cells was evaluated using the ImageJ software. An image was split into the color channels, then the contour of each cell was delimited using the freehand tool. The area, integrated density and mean grey value were measured for each cell in the image and in the background as well. The corrected total cell fluorescence (CTCF) was calculated as CTCF = Integrated Density – (Area of the selected cell × Mean grey value of background readings).

3. Results

3.1. Formation of histone *H2AX* phosphorylation foci (γH2AX) in human skin fibroblasts

As mentioned above, the measuring of histone H2AX phosphorylation on serine 139 is one of the most sensitive indicators of genotoxicity. In this study, we estimated the number of foci formed as a result of treating human skin fibroblasts with high-intensity THz radiation with various parameters.

The results of immunocytochemical staining of fibroblasts after the THz radiation exposure are displayed in Fig. 2; the dotted circle marks the area exposed to THz radiation. One can see that the number of foci may change from cell to cell. As mentioned earlier, it may be related both to the natural processes (cell cycle state, cellular senescence etc.) [30,31] and to the effect of the THz radiation. In this connection, we counted a relative number of foci in respect to the total number of irradiated cells. To eliminate possible risks associated with the individual specifics of cell cultures from different donors (gender, age, proliferative activity of cells etc.), we used cells of a 3^{d}-5^{th} passage from one and the same donor in all the experiments.

3.2. Time-effect plots of the THz radiation

One of the fundamental issues regarding the THz radiation safety for humans is the duration of exposure, as well as potential long-term effects of such a treatment. It has been shown, that various types of ionizing radiation can cause significant increase of γH2AX foci number in human cells. Due to the cell reparation system the number of γH2AX foci usually returns to the initial value within 24-72 hours post irradiation [23,47–49] Thus, not only the evaluation of γH2AX foci in the cells immediately after the THz exposure is of interest, but also changes in the γH2AX foci number occurring within a longer period of time post THz exposure. In our study, we decided to evaluate the γH2AX foci number at two time-points: immediately after the THz exposure and 24 hours post THz exposure.

Biomedical Optics EXPRESS

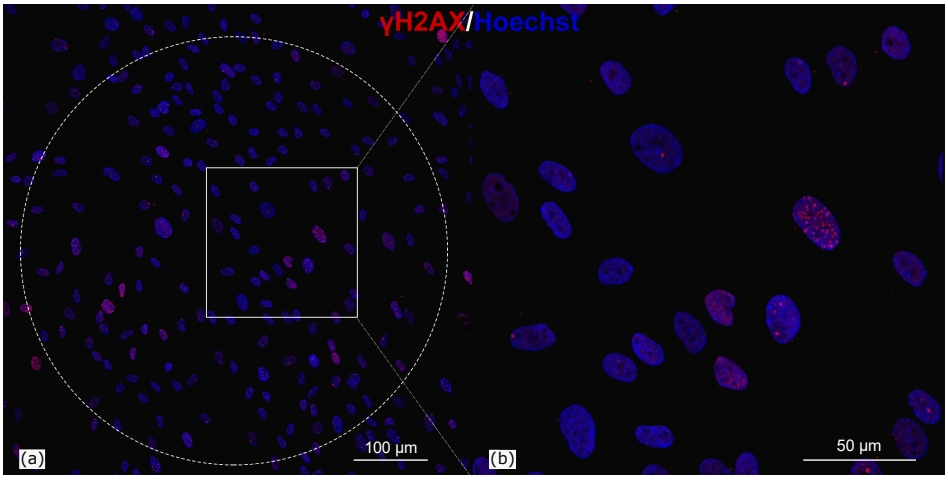

Fig. 2. Immunofluorescence analysis of γH2AX foci in human skin fibroblasts exposed to THz radication for 90 min and fixed on the next day after the irradiation. The area exposed to THz radiation is marked by the dotted circle. γH2AX were stained with goat-antirabbit secondary antibodies with Alexa Fluor 633 (red) and cell nuclei were stained with Hoechst (blue) in all panels. Scanning confocal microscopy. Bar size (a) 100 μm and (b) 50 μm.

A series of experiments was carried out at a preset THz pulse energy of $E^* = 15$ μJ, with the irradiation time t_i and the time after the radiation switch-off (so-called, fixing time) t_f. Figures 3(a) and 3(b) present the results of the study on the dynamics of formation of histone H2AX phosphorylation foci per one cell, $N_{f/c}$, after the treatment with high-intensity non-ionizing THz radiation for different times t_i. The quantification of γH2AX foci number in fibroblasts was performed directly after the exposure to THz radiation ($t_f = 0$ h, Fig. 3(a)) and 24 hours post THz radiation switch-off ($t_f = 24$ h, Fig. 3(b)).

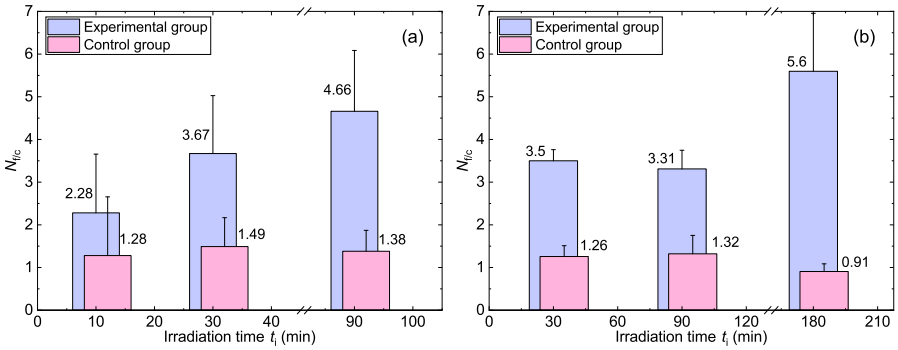

Fig. 3. Estimation of γH2AX foci number per cell in human skin fibroblasts: (a) immediately after the irradiation (t_f=0 h) and (b) 1 day after the irradiation (t_f=24 hrs) for different t_i times. p<0.05.

As seen from Fig. 3(a), the value of $N_{f/c}$ depends on the exposure duration and at $t_i > 30$ min the number of γH2AX foci in the experimental group substantially exceeds the corresponding value in the control group. Due to insignificant differences of $N_{f/c}$ in the experimental and control groups at $t_f = 0$ min we decided to exclude $t_i = 10$ min from the subsequent experiments. It is worth noticing that, in spite of the elevated number of γH2AX foci in the experimental group

Biomedical Optics EXPRESS

vs the control group at $t_i > 30$ min, neither foreign inclusions, nor morphological changes were observed in cells. The latter were assessed under the use of bright field microscopy (similar to [50]), taking into account the specific features of apoptotic or necrotic cells.

It is of interest that the numbers of γH2AX foci at $t_i = 30$ min and $t_i = 90$ min are not statistically different both immediately after the irradiation (Fig. 3(a)) and one day after the irradiation (Fig. 3(b)). Based on these data we may conclude, that the formation of γH2AX foci has a time-dependent effect, which persists for at least 24 hours in human fibroblasts. A time point of $t_i = 180$ min was added to the study for $t_f = 24$ hrs, since it demonstrated an essential increase in the number of γH2AX foci — by 6 times as compared to the parallel control group and by two times as compared to the results at $t_i = 30$ min and $t_i = 90$ min. However, even after the prolonged THz radiation treatment ($t_i = 180$ min) no morphological changes or signs of cell apoptosis were observed.

3.3. Determination of heat shock proteins in fibroblasts after the irradiation

One of the reasons for the formation of histone H2AX phosphorylation foci is the thermal effect on the cell [51]. THz radiation is strongly absorbed by water – the radiation power at a frequency of 1.5 THz drops by e times at a distance of ~30 μm. To estimate the increase in the temperature resulting from the absorption of continuous THz radiation of a given frequency and an average power, a theoretical model is conventionally used [52], based on the Kirchhoff equation for heat capacity. It was earlier shown [38,53] that pulsed THz radiation with the frequency υ=1.5 THz and the average power $P_{av} = E^*_{THz} \cdot f = 1.5$ mW (here $f = 100$ Hz and $E^*_{THz} = 15$ μJ is the energy of a THz pulse absorbed by water in a Petri dish), focused into a spot with the diameter of 480 μm resulted in the temperature increase ΔT=2.8°C in the beam center. The spatial distribution of temperature calculated with the use of the mentioned model [52] presented in Fig. 4 testifies the absence of significant heating.

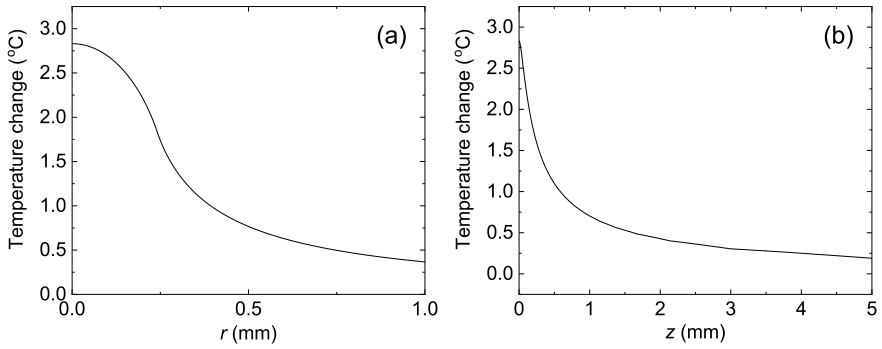

Fig. 4. Spatial distribution of temperature depending on (a) the radial coordinate r of the beam, (b) the axial coordinate z, directed into the aqueous medium.

Along with direct thermal imaging techniques applied in life science experiments [35,54], a number of studies utilized expression of heat shock proteins (HSP) for the thermal effect assessment [54,55]. For example, a study on the safety of microwave radiation used in the GSM mobile network [56] found an increase in the expression of heat shock proteins (HSP20, HSP27 and HSP70) after a 4-h-long treatment. It was also shown that the genes coding heat shock proteins, especially HSP40, HSP70 and HSP105, exhibit the highest expression immediately after the hyperthermic stress [57]. Besides, γH2AX foci can appear due to alternative mechanism of histone phosphorylation caused by rearrangement of chromatin as the result of thermal exposure [51,58].

Biomedical Optics EXPRESS

In this study, we evaluated the expression of heat shock proteins (HSP70) to test the hypothesis about the thermal origin of the observed increased number of γH2AX foci. The treatment of human skin fibroblasts was performed with THz radiation pulses of a preset energy $E^{*}_{\mathrm{THz}} = 15$ μJ with the duration of irradiation $t_{\mathrm{i}} = 30$ min.

The immunocytochemical analysis was performed for cells after the THz treatment (Fig. 5(a)) as well as for parallel (Fig. 5(c)) and positive (Fig. 5(d)) control groups. The corrected total cell fluorescence (CTCF) intensities for all the samples are presented in Fig. 5(e). No increase in the expression of heat shock proteins (HSP70) was observed in experimental group after irradiation for 30 min. On the other hand, when compared to the positive control (Fig. 5(d)), the expression of HSP70 in the experimental group was essentially lower. Data on additional temperatures of positive control can be found in Supplement 1. The Mann-Whitney test demonstrated the statistical difference between the positive control group and the rest of the groups while no difference was observed between the experimental and parallel control groups ($p<0.05$).

It is of note that histone H2AX phosphorylation foci were not associated with cells in which expression of HSP70 was observed (see white arrows in Fig. 5(c)). This finding does not agree with the idea of M. Blank [59] who considers HSP to be clearly indicative of mobilizing a defense mechanism, as they serve as biological markers for the cellular damage.

3.4. *Estimation of the influence of the oxidative stress caused by THz radiation on the proliferative index of human skin fibroblasts*

In spite of the fact that ROS are formed in a cell constantly, some exogenous factors (microwave, UV, heat action, chemicals etc.) may intensify formation of ROS. Exogenous ROS forms lead to destabilization of the chromatin structure, appearance of DNA DSB and cell apoptosis [60,61]. Such induced oxidative stress may also promote formation of γH2AX foci in a cell. While ionizing radiation directly damages DNA, NIR is believed to interfere with the oxidative repair mechanisms resulting in oxidative stress and leading to cancer through damaging cellular components including DNA [7,62].

In this study, we estimated the level of ROS after the THz radiation treatment of different duration (30, 90, and 180 min). As a positive control, the treatment of cells with hydrogen peroxide (H_2O_2) was used. The assessment of ROS was performed by immunofluorescence. The results of immunostaining of cells from the parallel control group, the experimental group exposed to THz radiation for 90 min and the positive control group labeled with CM-H2DCFDA are shown in Figs. 6(a)–(c) correspondingly. The corrected total cell fluorescence (CTCF) intensities for all the samples are presented in Fig. 6(d). The ROS levels in the experimental groups and the parallel control group were significantly lower as compared to the positive control group. The Mann-Whitney test demonstrated the statistical difference between the positive control group and the rest of the groups while no difference was observed between the experimental and parallel control groups ($p<0.05$)

The results of F-actin filaments staining by Phalloidin–Tetramethylrhodamine B isothiocyanate in the parallel control group, in the experimental group (exposed to THz radiation for 90 min), and in the positive control group are shown in Figs. 6(e)–(g) correspondingly. As can be seen, fibroblasts changed their typical spindle-shaped morphology into stellate-like morphology only in the positive control group. Such morphological changes are associated with microfilament reorganization due to disassembly of the F-actin cytoskeleton caused by H_2O_2 treatment. In the control group cells and cells after THz exposure the shape of microfilaments remained unchanged and the latter were observed as long stress fibers.

The formation of histone H2AX phosphorylation foci is frequently associated with disorders of the cell cycle that may lead to alterations in the proliferative activity of cells [31,34]. In this study, an estimation of cell proliferation was performed for different irradiation times t_{i}. In spite of the high intensity of the THz radiation and its prolonged action on human skin fibroblasts,

Biomedical Optics EXPRESS

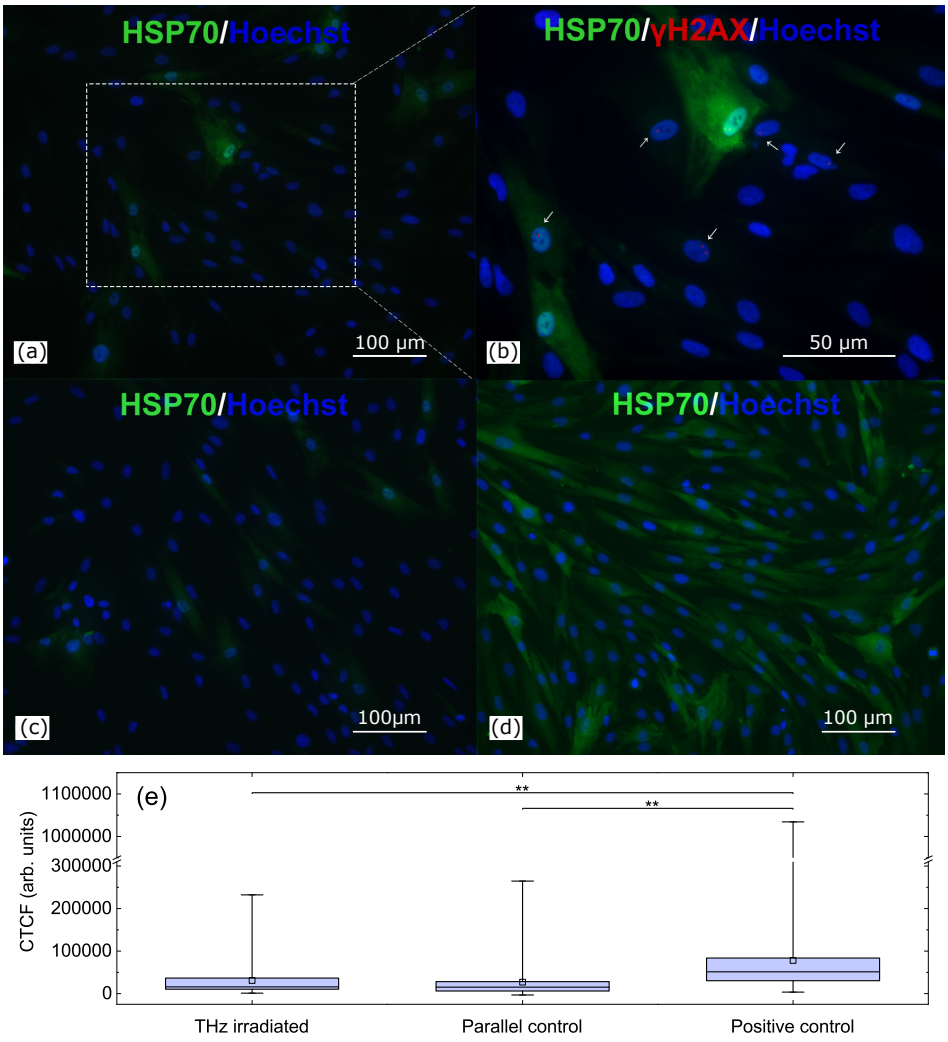

Fig. 5. Heat shock proteins expression in human skin fibroblasts after the THz exposure. (a) 30 min irradiation followed by fixation; (b) enlarged image of the irradiated field in panel (a), the arrows point to the foci of histone H2AX phosphorylation; (c) parallel control (cells not subjected to irradiation and thermal treatment); (d) cells after heating at 45°C (positive control); All groups are primary mouse anti-human HSP70 stained with secondary goat anti-mouse IgG (H + L) antibodies (green), primary rabbit anti-human γH2AX were stained with goat-antirabbit secondary antibodies with Alexa Fluor 633 ((b), red). Cell nuclei were stained with Hoechst (blue) in all panels. Scanning confocal microscopy; (e) mean fluorescence intensity of HSP70, $N>100$ cells/group. Asterisks indicate statistically significant difference (**$p<0.05$).

Biomedical Optics EXPRESS

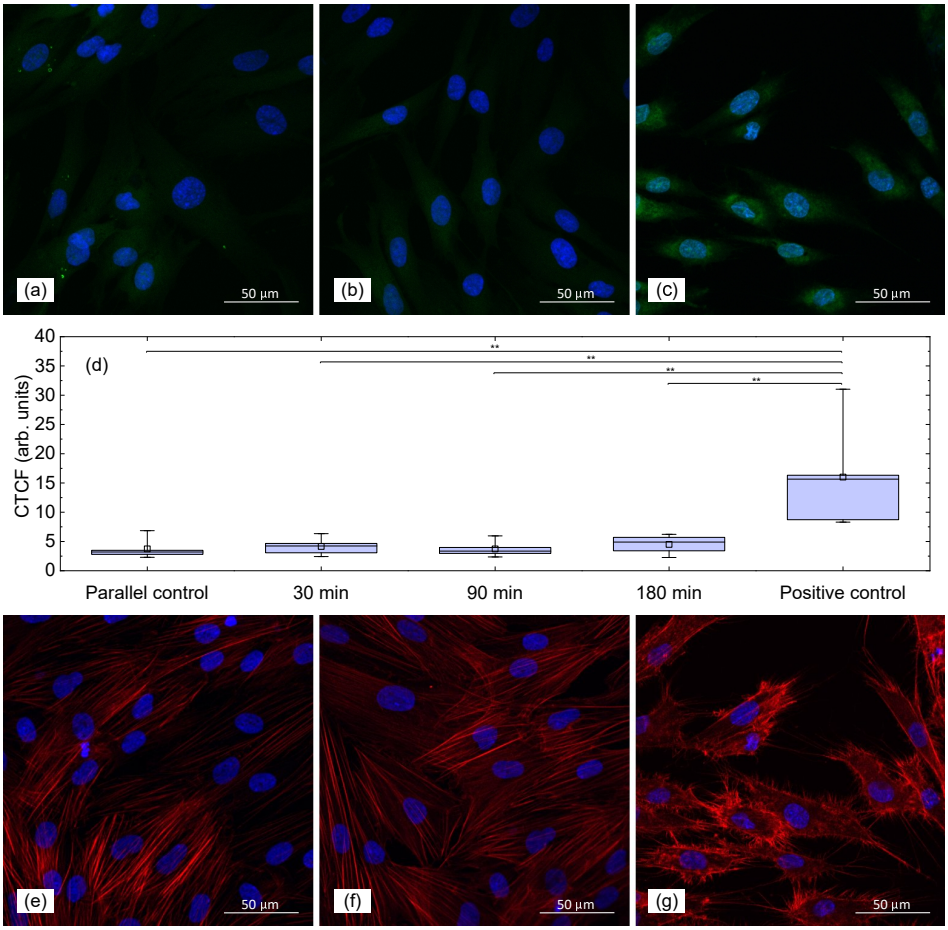

Fig. 6. Formation of ROS and actin filaments morphologies in human skin fibroblasts. ROS levels in (a) parallel control group, (b) experimental group exposed to THz radiation for 90 min, and (c) positive control group; (d) mean fluorescence intensity of ROS, (N>100 cells/group). Asterisks indicate statistically significant difference (**p<0.05). Morphology of actin filaments in human skin fibroblasts in (e) parallel control group, (f) experimental group exposed to THz radiation for 90 min, and (g) positive control group treated with H_2O_2. Cells were pre-loaded with CM-H2DCFDA (green) for ROS-detection in (a)–(c) panels; F-actin was stained with Phalloidin–Tetramethylrhodamine B isothiocyanate (orange) in (e)–(g) panels; cell nuclei were stained with Hoechst (blue) in all panels. Scanning confocal microscopy.

the number of cells expressing ki-67, as one of the proliferation markers, was approximately the same in all the experimental samples and did not differ from the control values. Besides, the proliferative index in all the cases was 50–65% that indicated the absence of any effect of THz radiation on cell proliferative activity (Fig. 7).

Biomedical Optics EXPRESS

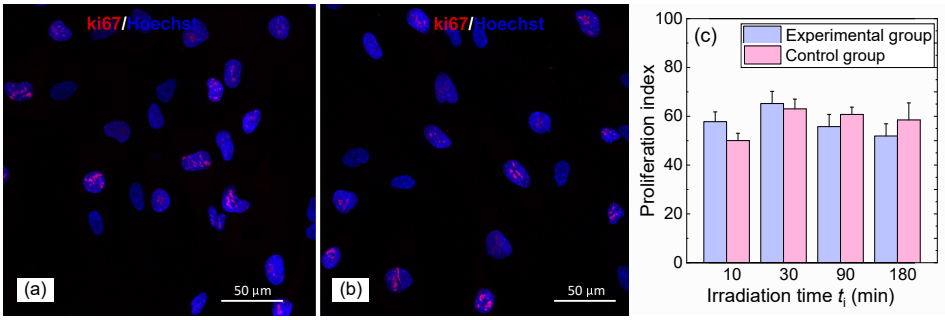

Fig. 7. Proliferative index supported by ki-67 in human skin fibroblasts in (a) the parallel control group and in (b) the experimental group exposed to THz radiation for 90 min; (c) bar diagram illustrating the % of the ki-67 positive cells in the experimental and parallel control groups. Cells were stained with primary rabbit polyclonal antibodies against ki-67 and secondary goat anti-rabbit antibodies conjugated with Alexa Fluor 633 (red). Cell nuclei were stained with Hoechst (blue). Scanning confocal microscopy.

4. Discussion

The formation of histone H2AX phosphorylation foci is one of the indicators of the genotoxic effect of different factors. In spite of the fact that the formation of these foci occurs spontaneously in the normal conditions, their number essentially grows in the presence of toxic agents. Histone H2AX phosphorylation resulting from the THz radiation treatment of different cell types have been studied earlier by several researchers. The parameters of the utilized THz radiation sources (frequency, average I_{av} and peak I_{peak} intensities) and the experimental conditions (time of exposure, temperature), significantly vary and are summarized in Table 1. As seen from Table 1, the induction of histone H2AX phosphorylation was found only in [33]. However, the performed analysis was qualitative and did not provide information on the quantitative changes of number of γH2AX foci in the experimental samples of artificial skin in comparison with the control samples.

In the study [34], quantitative analysis of the number of γH2AX foci was performed. Two experimental and two control Petri dishes with specimens of hESM01 human embryonic stem cell lines 2 hours post-irradiation were analyzed. It was shown that the mean number of γH2AX foci per nucleus for the two experimental groups was 4.1 ± 1.4 and comparable with the mean value for the two control groups, 3.7 ± 0.4. The absence of histone γH2AX phosphorylation resulting from THz irradiation of different fibroblast types was discussed in [35] and [28]. The authors conducted a quantitative analysis of the number of γH2AX foci; however, the data were presented in diagrams only, from which it was difficult to calculate the exact number of foci per cell. Nevertheless, one can see that the value varies from 0.3 to 1 on average and almost does not differ from the values in the control group.

In our study, we also estimate the formation of histone H2AX phosphorylation foci following the exposure of human skin fibroblasts to THz radiation. We used a significantly more powerful source of THz radiation (for similar values of the average power on the order of several mW, the peak intensity of the source we used was ~30 GW/cm^2, which was much higher than the values used in other studies). The data on the number of phosphorylation foci were obtained for several exposure times: 30, 90 and 180 min. Besides, in this study, in order to eliminate possible risks of an increase in the number of γH2AX foci associated with cellular senescence, we used cells of a 3^{d}-5th passage harvested from the one young and healthy donor in all the experiments.

Biomedical Optics EXPRESS

Table 1. Analysis of histone H2AX phosphorylation in response to THz radiation exposure

	Ref. [33]	Ref. [34]	Ref. [35]	Ref. [28]	This study
Sample	artificial human skin tissues equivalents	human embryonic stem cell line hESM01	human Fetal Foreskin Fibroblasts (HFFF2)	human adult dermal fibroblasts	human adult dermal fibroblasts
THz source	0.1-2 THz	2.3 THz	0.1-0.15 THz		0.1-3 THz
Repetition rate	1 kHz		2.5 Hz (for macropulse)		100 Hz
Pulse duration	~1.7 ps		4 μs[a]		0.5 ps
Exposure conditions	I_{av} = 57 mW/cm^2, I_{peak} = 66 MW/cm^2, W_{THz}[b] = 220 kV/cm, W_{THz}[c] = 70 kV/cm	I_{av} = 0.14 W/cm^2, I_{peak} = 4 kW/cm^2	I_{av} = 0.40 mW/cm^2, $P_{av} \leq$ 10 mW		I_{av}=0.84 mW/cm^2, I_{peak}=32 GW/cm^2
Exposure time	10 min	60 min	20 min		10, 30, 90, 180 min
Ambient temperature	21°C	24°C, cells were kept under 36.5–37.5•C	16°C	20°C	37°C
Temperature control	No	Yes, infrared imager	Yes, infrared camera		No
Expected temperature increase	ΔT = 0.7°C (calculated)		ΔT = 0.3°C (calculated)		ΔT = 2.8°C (calculated)
Type of analysis	Qualitative, immunochemical	Quantitative, Immunochemical	Quantitative, Immunochemical		Quantitative, Immunochemical
Time post exposure prior to analysis			30 min, 2 hrs, 24 hrs		0, 24 hrs
Induction of H2AX phosphorylation observed	Yes	No	No	No	Yes

[a]Each macropulse consists of 50 ps long micropulses with a 330 ps spacing between them
[b]"High" THz energy mode, E_{THz}=1 μJ
[c]"Low" THz energy mode – E_{THz}=0.1 μJ

We have demonstrated that the exposure to high-intensity THz radiation causes phosphorylation of the histone H2AX. It has been shown that the number of foci increases with the duration of irradiation and differs from that in the control groups. γH2AX phosphorylation foci are known to appear almost immediately after the exposure and their number reaches the highest values in 30 min [28,63]. Taking these findings into account, we have performed the analysis of γH2AX foci number formed one day after the irradiation. Foci formation in cells resulting from the THz exposure for 30 and 90 min is observed immediately after the end of irradiation and foci number remains at the same level on the next day.

Histone γH2AX phosphorylation has been considered earlier as an unambiguous marker of DNA DSB. However, evidences have been appearing currently that the presence of phosphorylation foci do not unequivocally testify the presence of DNA DSB. The study [64] demonstrated that the histone phosphorylation was unrelated to double-strand DNA breaks at relatively low levels of phosphorylation. Since histone γH2AX phosphorylation may be associated not only with the direct impact of THz radiation on DNA, but also with possible micro-heating or oxidative stress caused by THz radiation, we performed the corresponding analysis of these factors.

According to the results of our estimations, the temperature within the area of THz radiation focusing (with the average power of 1.5 mW) did not exceed 40°C. Such temperature elevation

Biomedical Optics EXPRESS

may lead to micro-heating of cells. The analysis of expression of heat shock proteins (chaperone proteins, participating in protein folding) within the field of THz radiation exposure may reveal the presence of such micro-heating regions. We performed a semi-quantitative immunochemical analysis of the most abundant heat shock protein with the molar mass of 70 kDa (HSP70). It was shown that the level of HSP70 expression in the THz radiation focus did not differ from that in the control group and was significantly lower than the level of HSP70 expression in the positive control cells. Besides, γH2AX foci were frequently found in cells not expressing heat shock proteins. However, since the analysis was semi-quantitative, we cannot confidently state that the THz radiation does not affect the genes responsible for the expression of chaperone proteins.

The ROS analysis has also demonstrated that THz irradiation does not result in the oxidative stress: the cells' morphology and cytoskeleton structure are preserved, and the amount of ROS does not exceed the control values. Even upon prolonged irradiation for 90 and 180 min, the ROS concentration did not increase. It should also be noted that the proliferative index of human skin fibroblasts, which underwent irradiation, did not differ from that measured in the control group and was about 50-65%.

Such results testify that non-ionizing THz radiation likely results in epigenetic genome alterations, which in turn may cause modification of the chromatin state or appearance of DNA DSB. While the formation of double-strand DNA breaks resulting from THz irradiation may be considered as disputable, the changes in the expression of certain genes caused by the THz irradiation has been repeatedly demonstrated [55,65–67]. In the studies [65,66] the THz radiation treatment led to a decreased level of expression of genes related to the epidermal differentiation complex in the chromosome region 1q21 (that opens opportunities for THz radiation application in therapeutic purposes to treat inflammatory and oncological skin diseases). In [67], abnormalities in the regulation of 8 signal pathways usually participating in initiation, sustaining, and progression of many human cancers were found, as well as altered expression of genes some of which were related to the regulation of tumor growth. In spite of the absence of direct DNA damage resulting from THz treatment, aneugenic effects of THz radiation have also been demonstrated [28,35,68,69]. The authors associated the genome damage with the induction of aneuploidy [28,35].

Thus, studying the safety of THz radiation is of great importance both for understanding the nature of NIR interaction with biological objects and for potential application of THz radiation sources. In our study, we have shown that even high-intensity THz radiation applied for a long time does not cause heating typical for other non-ionizing radiation types that, in turn, does not result in the oxidative stress in cells. The morphology and proliferative activity of cells were not affected. However, the increase in the number of H2AX histone phosphorylation foci testifies a possible genotoxic effect of THz radiation. Besides, the presence of large amount of residual γH2AX foci indicates a long-term effect of THz exposure, hence, it may be of an epigenetic character and increase the cells' sensitivity to other factors.

5. Conclusion

We have obtained new data on the effect of pulsed high-intensity THz radiation (with the intensity of ~30 GW/cm^2, the electric field strength of ~3.5 MV/cm) on human skin fibroblasts. It has been shown that the exposure of cells to high-intensity THz radiation does not affect their proliferative activity or morphology. However, such a treatment results in epigenetic changes of a cell due to histone H2AX phosphorylation. The formation of γH2AX foci has a time-dependent effect, which persists for at least 24 hours in human fibroblasts.

Funding. Russian Foundation for Basic Research (No. 19-02-00762).

Acknowledgments. The experiments were performed using the unique scientific facility "Terawatt Femtosecond Laser Complex" in the Center for Collective Usage "Femtosecond Laser Complex" of JIHT RAS. The reported study was funded by the Russian Fund for Basic Research (RFBR) according to the research project No. 19-02-00762.

Biomedical Optics EXPRESS

Disclosures. The authors declare no conflicts of interest.

Data availability. Data underlying the results presented in this paper are not publicly available at this time but may be obtained from the authors upon reasonable request.

Supplemental document. See Supplement 1 for supporting content.

References

1. K. Sulovská and M. Lehocký, "Terahertz spectroscopy characterization of antibacterial surfaces prepared via multistep physicochemical procedure," Opt. Eng. **54**(3), 034107 (2015).
2. K. I. Zaytsev, I. N. Dolganova, N. V. Chernomyrdin, G. M. Katyba, A. A. Gavdush, O. P. Cherkasova, G. A. Komandin, M. A. Shchedrina, A. N. Khodan, D. S. Ponomarev, I. V. Reshetov, V. E. Karasik, M. Skorobogatiy, V. N. Kurlov, and V. V. Tuchin, "The progress and perspectives of terahertz technology for diagnosis of neoplasms: a review," J. Opt. **22**(1), 013001 (2020).
3. A. A. Gavdush, N. V. Chernomyrdin, G. A. Komandin, I. N. Dolganova, P. V. Nikitin, G. R. Musina, G. M. Katyba, A. S. Kucheryavenko, I. V. Reshetov, A. A. Potapov, V. V. Tuchin, and K. I. Zaytsev, "Terahertz dielectric spectroscopy of human brain gliomas and intact tissues ex vivo: double-Debye and double-overdamped-oscillator models of dielectric response," Biomed. Opt. Express **12**(1), 69–83 (2021).
4. A. I. Nikitkina, P. Y. Bikmulina, E. R. Gafarova, N. V. Kosheleva, Y. M. Efremov, E. A. Bezrukov, D. V. Butnaru, I. N. Dolganova, N. V. Chernomyrdin, O. P. Cherkasova, A. A. Gavdush, and P. S. Timashev, "Terahertz radiation and the skin: a review," J. Biomed. Opt. **26**(04), 043005 (2021).
5. Y. Zou, Q. Liu, X. Yang, H.-C. Huang, J. Li, L.-H. Du, Z.-R. Li, J. J.-H. Zhao, and L. L.-G. Zhu, "Label-free monitoring of cell death induced by oxidative stress in living human cells using terahertz ATR spectroscopy," Biomed. Opt. Express **9**(1), 14–24 (2018).
6. L. Yu, L. Hao, T. Meiqiong, H. Jiaoqi, L. Wei, D. Jinying, C. Xueping, F. Weiling, and Z. Yang, "The medical application of terahertz technology in non-invasive detection of cells and tissues: opportunities and challenges," RSC Adv. **9**(17), 9354–9363 (2019).
7. M. Havas, "When theory and observation collide: Can non-ionizing radiation cause cancer?" Environmental Pollution **221**, 501–505 (2017).
8. D. Belpomme, L. Hardell, I. Belyaev, E. Burgio, and D. O. Carpenter, "Thermal and non-thermal health effects of low intensity non-ionizing radiation: An international perspective," Environmental Pollution **242**, 643–658 (2018).
9. H. Hintzsche and H. Stopper, "Effects of terahertz radiation on biological systems," Crit. Rev. Environ. Sci. Technol. **42**(22), 2408–2434 (2012).
10. G. J. Wilmink and J. E. Grundt, "Invited review article: Current state of research on biological effects of terahertz radiation," J. Infrared, Millimeter, Terahertz Waves **32**(10), 1074–1122 (2011).
11. V. I. Fëdorov, D. S. Serdyukov, O. P. Cherkasova, S. S. Popova, and E. F. Nemova, "The influence of terahertz radiation on the cell's genetic apparatus," J. Opt. Technol. **84**(8), 509–514 (2017).
12. M. Borovkova, M. Serebriakova, V. Fedorov, E. Sedykh, V. Vaks, A. Lichutin, A. Salnikova, and M. Khodzitsky, "Investigation of terahertz radiation influence on rat glial cells," Biomed. Opt. Express **8**(1), 273–280 (2017).
13. I. V. Il'ina, D. S. Sitnikov, and M. B. Agranat, "State-of-the-art of studies of the effect of terahertz radiation on living biological systems," High Temp. **56**(5), 789–810 (2018).
14. H. Cheon, H.-J. Yang, M. Choi, and J.-H. Son, "Effective demethylation of melanoma cells using terahertz radiation," Biomed. Opt. Express **10**(10), 4931–4941 (2019).
15. O. P. Cherkasova, D. S. Serdyukov, A. S. Ratushnyak, E. F. Nemova, E. N. Kozlov, Y. V. Shidlovskii, K. I. Zaytsev, and V. V. Tuchin, "Effects of terahertz radiation on living cells: a review," Opt. Spectrosc. **128**(6), 855–866 (2020).
16. D. S. Serdyukov, T. N. Goryachkovskaya, I. A. Mescheryakova, S. V. Bannikova, S. A. Kuznetsov, O. P. Cherkasova, V. M. Popik, and S. E. Peltek, "Study on the effects of terahertz radiation on gene networks of Escherichia coli by means of fluorescent biosensors," Biomed. Opt. Express **11**(9), 5258–5273 (2020).
17. S. Shang, X. Wu, Q. Zhang, J. Zhao, E. Hu, L. Wang, and X. Lu, "0.1 THz exposure affects primary hippocampus neuron gene expression via alternating transcription factor binding," Biomed. Opt. Express **12**(6), 3729–3742 (2021).
18. B. S. Alexandrov, V. Gelev, A. R. Bishop, A. Usheva, and K. Ø. Rasmussen, "DNA breathing dynamics in the presence of a terahertz field," Phys. Lett. A **374**(10), 1214–1217 (2010).
19. B. Kopp, L. Khoury, and M. Audebert, "Validation of the γH2AX biomarker for genotoxicity assessment: a review," Arch. Toxicol. **93**(8), 2103–2114 (2019).
20. G. G. Wang, C. D. Allis, and P. Chi, "Chromatin remodeling and cancer, part I: covalent histone modifications," Trends Mol. Med. **13**(9), 363–372 (2007).
21. E. P. Rogakou, D. R. Pilch, A. H. Orr, V. S. Ivanova, and W. M. Bonner, "DNA double-stranded breaks induce histone H2AX phosphorylation on serine 139," J. Biol. Chem. **273**(10), 5858–5868 (1998).
22. N. S. Bicheru, C. Haidoiu, O. Călborean, A. Popa, I. Porosnicu, and R. Hertzog, "Effect of different antioxidants on X-ray induced DNA double-strand breaks using γ-H2AX in human blood lymphocytes," Health Phys. **119**(1), 101–108 (2020).
23. N. Babayan, B. Grigoryan, L. Khondkaryan, G. Tadevosyan, N. Sarkisyan, R. Grigoryan, L. Apresyan, R. Aroutiounian, N. Vorobyeva, M. Pustovalova, A. Grekhova, and A. N. Osipov, "Laser-driven ultrashort pulsed electron beam radiation at doses of 0.5 and 1.0 Gy induces apoptosis in human fibroblasts," Int. J. Mol. Sci. 20(20), 5140 (2019).

Biomedical Optics EXPRESS

24. A. N. Osipov, M. Pustovalova, A. Grekhova, P. Eremin, N. Vorobyova, A. Pulin, A. Zhavoronkov, S. Roumiantsev, D. Y. Klokov, and I. Eremin, "Low doses of X-rays induce prolonged and ATM-independent persistence of γH2AX foci in human gingival mesenchymal stem cells," Oncotarget **6**(29), 27275–27287 (2015).
25. T. Sugihara, H. Murano, and K. Tanaka, "Increased γ-H2A.X intensity in response to chronic medium-dose-rate γ-ray irradiation," PLoS One **7**(9), e45320 (2012).
26. S. de Feraudy, I. Revet, V. Bezrookove, L. Feeney, and J. E. Cleaver, "A minority of foci or pan-nuclear apoptotic staining of H2AX in the S phase after UV damage contain DNA double-strand breaks," Proc. Natl. Acad. Sci. **107**(15), 6870–6875 (2010).
27. J. E. Cleaver, "γH2Ax: Biomarker of damage or functional participant in DNA repair "All that glitters is not gold!" Photochem. Photobiol. **87**(6), 1230–1239 (2011).
28. V. Franchini, S. De Sanctis, J. Marinaccio, A. De Amicis, E. Coluzzi, S. Di Cristofaro, F. Lista, E. Regalbuto, A. Doria, E. Giovenale, G. P. Gallerano, R. Bei, M. Benvenuto, L. Masuelli, I. Udroiu, and A. Sgura, "Study of the effects of 0.15 terahertz radiation on genome integrity of adult fibroblasts," Environ. Mol. Mutagen. **59**(6), 476–487 (2018).
29. S. Dhuppar, S. Roy, and A. Mazumder, "γH2AX in the S phase after UV irradiation corresponds to DNA replication and does not report on the extent of DNA damage," Mol. Cell. Biol. **40**(20), e00328 (2020).
30. E. Mejia-Ramirez, O. Limbo, P. Langerak, and P. Russell, "Critical function of γH2A in S-phase," PLoS Genet **11**(9), e1005517 (2015).
31. V. Zorin, A. Grekhova, M. Pustovalova, A. Zorina, N. Smetanina, N. Vorobyeva, P. Kopnin, I. Gilmutdinova, A. Moskalev, A. N. Osipov, and S. Leonov, "Spontaneous γH2AX foci in human dermal fibroblasts in relation to proliferation activity and aging," Aging **11**(13), 4536–4546 (2019).
32. T. Katsube, M. Mori, H. Tsuji, T. Shiomi, B. Wang, Q. Liu, M. Nenoi, and M. Onoda, "Most hydrogen peroxide-induced histone H2AX phosphorylation is mediated by ATR and is not dependent on DNA double-strand breaks," J. Biochem. **156**(2), 85–95 (2014).
33. L. V. Titova, A. K. Ayesheshim, A. Golubov, D. Fogen, R. Rodriguez-Juarez, F. A. Hegmann, and O. Kovalchuk, "Intense THz pulses cause H2AX phosphorylation and activate DNA damage response in human skin tissue," Biomed. Opt. Express **4**(4), 559–568 (2013).
34. A. N. Bogomazova, E. M. Vassina, T. N. Goryachkovskaya, V. M. Popik, A. S. Sokolov, N. A. Kolchanov, M. A. Lagarkova, S. L. Kiselev, and S. E. Peltek, "No DNA damage response and negligible genome-wide transcriptional changes in human embryonic stem cells exposed to terahertz radiation," Sci. Rep. **5**(1), 7749 (2015).
35. A. De Amicis, S. De Sanctis, S. Di Cristofaro, V. Franchini, F. Lista, E. Regalbuto, E. Giovenale, G. P. Gallerano, P. Nenzi, R. Bei, M. Fantini, M. Benvenuto, L. Masuelli, E. Coluzzi, C. Cicia, and A. Sgura, "Biological effects of in vitro THz radiation exposure in human foetal fibroblasts," Mutation Research/Genetic Toxicology and Environmental Mutagenesis **793**, 150–160 (2015).
36. C. Vicario, M. Jazbinsek, A. V. Ovchinnikov, O. V. Chefonov, S. I. Ashitkov, M. B. Agranat, and C. P. Hauri, "High efficiency THz generation in DSTMS, DAST and OH1 pumped by Cr:forsterite laser," Opt. Express **23**(4), 4573–4580 (2015).
37. A. V Ovchinnikov, O. V Chefonov, D. S. Sitnikov, I. V Il'ina, S. I. Ashitkov, and M. B. Agranat, "A source of THz radiation with electric field strength of more than 1 MV/cm on the basis of 100-Hz femtosecond Cr:forsterite laser system," Quantum Electron. **48**(6), 554–558 (2018).
38. D. S. Sitnikov, I. V Ilina, and A. A. Pronkin, "Experimental system for studying bioeffects of intense terahertz pulses with electric field strength up to 3.5 MV/cm," Opt. Eng. **59**(06), 1 (2020).
39. D. S. Sitnikov, S. A. Romashevskiy, A. V Ovchinnikov, O. V Chefonov, A. B. Savel'ev, and M. B. Agranat, "Estimation of THz field strength by an electro-optic sampling technique using arbitrary long gating pulses," Laser Phys. Lett. **16**(11), 115302 (2019).
40. A. I. Shpichka, V. A. Revkova, N. A. Aksenova, G. M. Yusubalieva, V. A. Kalsin, E. F. Semenova, Y. Zhang, V. P. Baklaushev, and P. S. Timashev, "Transparent PEG-Fibrin Gel as a Flexible Tool for Cell Encapsulation," Sovrem Tehnol Med **10**(1), 64–69 (2018).
41. D. Sitnikov, I. Ilina, O. Chefonov, A. Ovchinnikov, V. Revkova, M. Konoplyannikov, V. Kalsin, and V. Balkaushev, "Double-stand DNA foci formation in human skin fibroblasts after high-power THz pulses exposure," Proc. SPIE **11582**, 1158204 (2020).
42. M. Ayuso, S. Van Cruchten, and C. Van Ginneken, "A medium-throughput system for in vitro oxidative stress assessment in IPEC-J2 cells," Int. J. Mol. Sci. **21**(19), 7263 (2020).
43. T. Sieprath, T. Corne, J. Robijns, W. J. H. Koopman, and W. H. De Vos, "Cellular redox profiling using high-content microscopy," JoVE **123**, e55449 (2017).
44. C.-Y. Hsieh, C.-L. Chen, K.-C. Yang, C.-T. Ma, P.-C. Choi, and C.-F. Lin, "Detection of reactive oxygen species during the cell cycle under normal culture conditions using a modified fixed-sample staining method," Journal of Immunoassay and Immunochemistry **36**(2), 149–161 (2015).
45. R. Sales Gil and P. Vagnarelli, "Ki-67: more hidden behind a 'classic proliferation marker'," Trends Biochem. Sci. **43**(10), 747–748 (2018).
46. I. Miller, M. Min, C. Yang, C. Tian, S. Gookin, D. Carter, and S. L. Spencer, "Ki67 is a graded rather than a binary marker of proliferation versus quiescence," Cell Rep. **24**(5), 1105–1112.e5 (2018).

Biomedical Optics EXPRESS

47. A. Liubavičiūtė, J. A. Kraśko, A. Mlynska, J. Lagzdina, K. Sužiedėlis, and V. Pašukonienė, "Evaluation of low-dose proton beam radiation efficiency in MIA PaCa-2 pancreatic cancer cell line vitality and H2AX formation," Medicina **51**(5), 302–306 (2015).
48. N. Babayan, N. Vorobyeva, B. Grigoryan, A. Grekhova, M. Pustovalova, S. Rodneva, Y. Fedotov, G. Tsakanova, R. Aroutiounian, and A. Osipov, "Low repair capacity of DNA double-strand breaks induced by laser-driven ultrashort electron beams in cancer cells," J. Phys.: Conf. Ser. **21**(24), 9488 (2020).
49. M. Pustovalova, L. Alhaddad, N. Smetanina, A. Chigasova, T. Blokhina, R. Chuprov-Netochin, A. N. Osipov, and S. Leonov, "The p53–53BP1-related survival of A549 and H1299 human lung cancer cells after multifractionated radiotherapy demonstrated different response to additional acute X-ray exposure," Int. J. Mol. Sci. 21(9), 3342 (2020).
50. D. S. Sitnikov, I. V. Ilina, A. A. Pronkin, A. V. Ovchinnikov, O. V. Chefonov, I. M. Zurina, A. A. Gorkun, and N. V. Kosheleva, "Studying the effect of high-power coherent terahertz pulses on mesenchymal stem cells," J. Phys. Conf. Ser. **1147**, 012060 (2019).
51. A. Laszlo and I. Fleischer, "The heat-induced -H2AX response does not play a role in hyperthermic cell killing," International Journal of Hyperthermia **25**(3), 199–209 (2009).
52. T. T. Kristensen, W. Withayachumnankul, P. U. Jepsen, and D. Abbott, "Modeling terahertz heating effects on water," Opt. Express **18**(5), 4727–4739 (2010).
53. D. S. Sitnikov, A. A. Pronkin, I. V. Ilina, V. A. Revkova, M. A. Konoplyannikov, V. A. Kalsin, and V. P. Baklaushev, "Numerical modelling and experimental verification of thermal effects in living cells exposed to high-power pulses of THz radiation," Sci. Rep. **11**(1), 17916 (2021).
54. B. S. Alexandrov, K. Ø. Rasmussen, A. R. Bishop, A. Usheva, L. B. Alexandrov, S. Chong, Y. Dagon, L. G. Booshehri, C. H. Mielke, M. L. Phipps, J. S. Martinez, H.-T. Chen, and G. Rodriguez, "Non-thermal effects of terahertz radiation on gene expression in mouse stem cells," Biomed. Opt. Express **2**(9), 2679–2689 (2011).
55. I. Echchgadda, C. Z. Cerna, M. a. Sloan, D. P. Elam, and B. L. Ibey, "Effects of different terahertz frequencies on gene expression in human keratinocytes," Proc. SPIE **9321**, 93210Q (2015).
56. E. Calabrò, "Modulation of heat shock protein response in SH-SY5Y by mobile phone microwaves," WJBC **3**(2), 34–40 (2012).
57. I. Echchgadda, C. Roth, C. Cerna, and G. Wilmink, "Temporal gene expression kinetics for human keratinocytes exposed to hyperthermic stress," Cells **2**(2), 224–243 (2013).
58. J. L. Roti Roti, R. K. Pandita, J. D. Mueller, P. Novak, E. G. Moros, and A. Laszlo, "Severe, short-duration (0-3 min) heat shocks (50-52°C) inhibit the repair of DNA damage," International Journal of Hyperthermia **26**(1), 67–78 (2010).
59. M. Blank, "Non-ionizing radiation (NIR): evaluating safety," Environmental Pollution **222**, 153 (2017).
60. T. Finkel and N. J. Holbrook, "Oxidants, oxidative stress and the biology of ageing," Nature **408**(6809), 239–247 (2000).
61. C. Bertram and R. Hass, "Cellular responses to reactive oxygen species-induced DNA damage and aging," Biol. Chem. **389**(3), 211–220 (2008).
62. A. K. Dharmadhikari, H. Bharambe, J. A. Dharmadhikari, J. S. D'Souza, and D. Mathur, "DNA damage by OH radicals produced using intense, ultrashort, long wavelength laser pulses," Phys. Rev. Lett. **112**(13), 138105 (2014).
63. O. A. Sedelnikova, D. R. Pilch, C. Redon, and W. M. Bonner, "Histone H2AX in DNA damage and repair," Cancer Biol. Ther. **2**(3), 233–235 (2003).
64. P. Rybak, A. Hoang, L. Bujnowicz, T. Bernas, K. Berniak, M. Zarębski, Z. Darzynkiewicz, and J. Dobrucki, "Low level phosphorylation of histone H2AX on serine 139 (γH2AX) is not associated with DNA double-strand breaks," Oncotarget **7**(31), 49574–49587 (2016).
65. L. V. Titova, A. K. Ayesheshim, A. Golubov, R. Rodriguez-Juarez, R. Woycicki, F. A. Hegmann, and O. Kovalchuk, "Intense THz pulses down-regulate genes associated with skin cancer and psoriasis: a new therapeutic avenue?" Sci. Rep. **3**(1), 2363 (2013).
66. L. V. Titova, A. K. Ayesheshim, A. Golubov, R. Rodriguez-Juarez, A. Kovalchuk, F. A. Hegmann, and O. Kovalchuk, "Intense picosecond THz pulses alter gene expression in human skin tissue in vivo," Proc. SPIE **8585**, 85850Q (2013).
67. C. M. Hough, D. N. Purschke, C. Huang, L. V Titova, O. V Kovalchuk, B. J. Warkentin, and F. A. Hegmann, "Intense terahertz pulses inhibit Ras signaling and other cancer-associated signaling pathways in human skin tissue models," J. Phys. Photonics **3**(3), 034004 (2021).
68. A. Korenstein-Ilan, A. Barbul, P. Hasin, A. Eliran, A. Gover, and R. Korenstein, "Terahertz radiation increases genomic instability in human lymphocytes," Radiat. Res. **170**(2), 224–234 (2008).
69. H. Hintzsche, C. Jastrow, T. Kleine-Ostmann, H. Stopper, E. Schmid, and T. Schrader, "Terahertz radiation induces spindle disturbances in human-hamster hybrid cells," Radiat. Res. **175**(5), 569–574 (2011).